Available online at www.sciencedirect.com
SCIENCE DIRECT®
Radiation Physics and Chemistry 70 (2004) 191–206
Radiation Physics and Chemistry
www.elsevier.com/locate/radphyschem

Double ionization by one and many photons

Reinhard Dörner*, Horst Schmidt-Böcking, Thorsten Weber, Till Jahnke, Markus Schöffler, Alexandra Knapp, Mirko Hattass, Achim Czasch, Lothar Ph. H. Schmidt, Ottmar Jagutzki

Institut für Kernphysik, Universität Frankfurt, Frankfurt D-60486, Germany

Abstract

This paper describes the mechanisms by which the nonresonant interaction of photons with atoms can lead to direct emission of two electrons from an atom. We discuss three different light-matter interactions: absorption of one (high energy) photon, Compton scattering of one photon (in both cases utilizing synchrotron radiation) and multiphoton processes in strong femtosecond laser fields. From a mainly experimental and phenomenological perspective the interaction mechanisms and their experimental evidences are discussed.

Keywords: Photoionization; Helium; Double ionization; Compton scattering; Multiphoton ionization; COLTRIMS; Three body problem; Strong field ionization; Rescattering; Shake off

1. Introduction

The dynamics of few-body systems is still one of the great challenges in physics. It is of central importance in many fields of physics from solid state to nuclear physics. A particularly clean way to address this problem is the investigation of double ejection of electrons from atoms induced by interaction with light. This interaction can be the absorption of a single photon, Compton scattering and ionization in a strong laser field by absorption of many low energy photons. In all three cases the energy deposited in an atom can lead to ejection of more than one electron. What are the similarities and differences in these double ionization processes? What is the probability for the emission of the second electron and what are the mechanisms by which it is ejected? What is the final state momentum distribution? These are some of the question we will address in this review.

Very different level of detail in the experiments and in our understanding has been reached in the three fields. Double ionization by single photon absorption has been investigated mostly for He as the most simple two electron system. Here a high level of detail has been reached and only a few questions remain open. Fully differential cross sections as well as precise total cross section have been reported for the full energy range from threshold (79 eV) to 550 eV photon energy for both, linear and circular polarized light. The fully differential cross sections have been reviewed recently by Briggs and Schmidt (2000). For double ionization by Compton scattering in contrast the experimental data are scarce and from theory side most of the studies deal with total cross sections only. Double ionization in strong fields is the youngest of the fields. Here tremendous experimental progress has been made in the recent 3 years. However, much remains to be done experimentally as well as theoretically. A recent review covering this emerging field can be found in Dörner et al. (2002).

Section 2 deals with a cross comparison between single ionization caused by single photoabsorption, Compton scattering and multiphoton absorption. Section 3 describes mechanisms by which double ionization can occur. Sections 4–6.4 deal with some of the key findings for each double ionization process. Section 7 draws some lines comparing double ionization from the three light matter interaction processes and highlights the open questions.

*Corresponding author.
E-mail address: doerner@hsb.uni-frankfurt.de (R. Dörner).

0969-806X/$ - see front matter © 2003 Elsevier Ltd. All rights reserved.
doi:10.1016/j.radphyschem.2003.12.012

2. Comparison of photoabsorption, Compton scattering and strong field ionization

What are the main similarities and differences between the single ionization of an atom by absorption of one photon, Compton scattering or by absorption of many photons in a strong laser field? Some of the important features of the three interactions can be seen from the data shown in Fig. 1. In all cases the momentum distribution of He^{1+} ions is presented. The light is linear polarized along the horizontal axis. For single and multi photon absorption, the ion momentum distributions are an almost exact mirror image of the electron momenta. This follows from momentum conservation since the momentum of the photon can be neglected in both cases. For Compton scattering in contrast the momentum of the ejected electron is balanced by the scattered high energy photon, the recoiling ion is only a spectator and hence carries very little momentum. This ion momentum results from the initial state momentum wavefunction (Compton profile). For single photon absorption the electron energy is given by $E_e = E_\gamma - E_{bind} - E_{exc}$, where E_{bind} is the ionization potential and E_{exc} is excitation energy in the remaining singly charged ion, e.g. $E_{exc} = 0$ for the ionic ground state. Consequently, the momentum vectors in Fig. 1(a) all end on spheres, the outer sphere corresponds to the He^{1+} ground state. In this sense photoabsorption creates relatively hot ions. The rim in Fig. 1(b) also results from photoabsorption while the narrow peak at zero momentum are ions created by Compton scattering. For strong field ionization the momentum distribution of the ions and electrons is very narrow directed along the polarization axis. 10^{15} W/cm^2 corresponds to about 10^9 coherent photons in a box of the size of the wavelength (800 nm). Such densities of coherent photons in the laser pulse suggests a change from the "photon-" to the "field-perspective". The laser field can be described as a classical electromagnetic field, neglecting the quantum nature of the photons. From this point of view the relevant quantities are the field strength and its frequency. 10^{16} W/cm^2 at 800 nm corresponds to a field of 3×10^{11} V/m comparable to the field experienced by the electron on a Bohr orbit in atomic hydrogen (5×10^{11} V/m).

How do the ions and electrons get their momentum in the three processes? For the case of single photon absorption the light field is so weak that there is no external acceleration. Also the photon carries no significant momentum into the reaction. The momenta observed in the final state thus have to be present already in the initial state of the atom. The photon cuts the tie between nucleus and electron by providing the energy, the momentum however was present already in the initial state Compton profile. Single photon absorption is therefore linked to a particular fraction of the initial state wave function which in momentum representation coincides with the final state momentum (see Fig. 2). In the coordinate space representation this fraction of the wave function is confined close to the nucleus. The scaling of the photo ionization cross

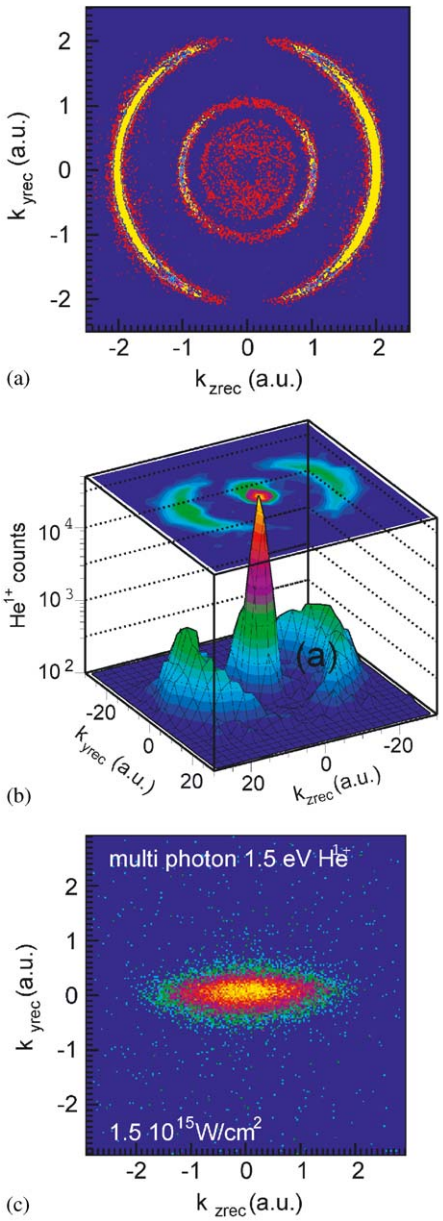

Fig. 1. Momentum distributions of singly charged ions. The polarization axis is along k_{zrec}. (a) single photon absorption, 80 eV photons. The rings correspond to different electronic states of the He^{1+} ions. (b) 7 keV photons (outer rim: absorption, narrow peak: Compton scattering). (c) TiSa laser pulse 1.5 eV (800 nm), 220 fs, 1.4×10^{15} W/cm^2. (a) shows a narrow slice through the three-dimensional momentum space, (b) and (c) are integrated over the third dimension.

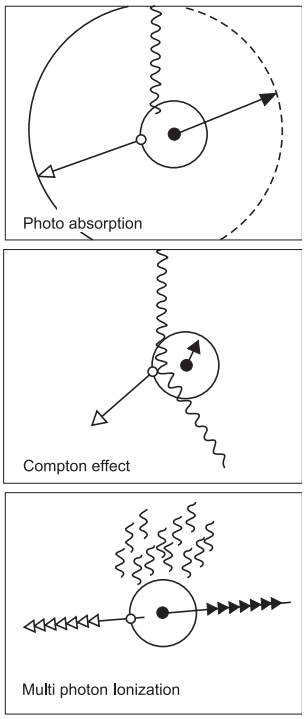

Fig. 2. Schematic view of the ionization by single photon absorption, Compton scattering and in a strong laser field.

section at high energies simply follows the initial state momentum space Compton profile, i.e. the probability to find an electron–ion pair with the appropriate momentum in the initial state. For Compton scattering as discussed above the ion momentum is mainly the initial state momentum, the electron momentum is given by the binary collision of the photon with the electron smeared by the initial state electron momentum. In the strong field case finally the field is strong enough to accelerate the ions and electrons substantially after the electron is set free. The momentum balance however is still the same as in the single photon limit: The laser field accelerates electron and ion to the opposite directions resulting again in their back-to-back emission. This changes only if the laser pulse is long enough that the electron can escape from the focus during pulse duration. In this case, which we do not consider here, the momenta are balanced by a huge amount of elastically scattered photons. In the regime of wavelength and binding energies under consideration here, a simple two-step picture has been proven useful. In the first step the electron is set free by tunneling through the potential barrier created by the superposition of the Coulomb potential of the atom and the electric field of the laser. This process promotes electrons and ions with zero momentum to the continuum. They are subsequently accelerated in the laser field and perform a quiver motion. The net momentum which is observed after the pulse with envelope of the electric field strength $E(t)$ is in this model purely a function of the phase of the field at the instant of tunneling (tunneling time t_0) (atomic units are used throughout this paper):

$$p_z^{\mathrm{He}^{1+}}(t_\infty) = \int_{t_0}^{t_\infty} E(t) \sin \omega t \, \mathrm{d}t. \quad (1)$$

Tunneling at the field maximum thus leads to electrons and ions with zero momentum. The maximum momentum corresponding to the zero crossing of the laser field is $\sqrt{4U_\mathrm{p}}$, where $U_\mathrm{p} = I/4\omega^2$ is the ponderomotive potential at an intensity I and the photon frequency ω ($U_\mathrm{P} = 39.4$ eV at 6.6×10^{14} W/cm^2). It is important to note that within this simplified picture the ion momentum measurement corresponds directly to a time measurement.

3. Mechanisms of double ionization

For the three interactions discussed in the previous section one observes a probability of up to a few percent that two electrons are ejected whenever this is energetically allowed. What are the "mechanisms" leading to double ionization? This seemingly clear-cut question does not necessarily have a quantum mechanical answer. The word "mechanism" mostly refers to an intuitive mechanistical picture. It is not always clear how this intuition can be translated into theory and even if one finds such a translation the contributions from different mechanisms have to be added coherently to obtain the measurable final state of the reaction (Ken-ichi Hino et al., 1993; Kheifets, 2001). Thus, only in some cases mechanisms are experimentally accessible. This is only the case if different mechanisms occur at different strengths of the perturbation (such as laser power or projectile charge) or if they predominantly populate different regions of the final state phase space. In these cases situations can be found where one mechanism dominates such that interference becomes negligible. Adding to these complication is that within different theoretical approaches the same word (e.g. shake-off) has different meaning and even within the same approach the relative contributions of the mechanisms are sometimes gauge dependent. A very helpful cross comparison between different theoretical usage of the terms introduced below can be found in Schneider and Rost (2003). With these words of caution in mind, we list the most discussed mechanisms leading to double ionization. Some of them are common between the different forms of light-matter interaction some are possible only in special cases.

1. *Two-step-two* (*TS2*) *or sequential ionization*: Here the two electrons are emitted sequentially by two independent interactions of the light field with the

atom. In the case of single photon absorption this is impossible. For Compton scattering it corresponds to a double Compton scattering of one photon consecutively at two electrons of the same atom. Given the typical area of an atom of 10^{-16} cm^2 and a typical cross section for Compton scattering of 10^{-24} cm^2 one can estimated the cross section for double Compton scattering to be in the range of 10^{-30} cm^2 and thus completely irrelevant for the present discussion. For the strong field ionization however this is an important process. Here one could say from a photon perspective that each of the electrons absorbs photons independently. From the field perspective one would say that each electron tunnels independently at different times during the laser pulse. This is equivalent to the TS2 mechanism in ion–atom and electron–atom collisions. In this approximation the probability of the double ejection can be estimated in an independent particle model. Most simply one calculates double ionization as two independent steps of single ionization. A little more refined approach uses an independent event model, which takes into account the different binding energies for the ejection of the first and the second electron (see e.g. Shingal and Lin, 1991 for ion impact; Lambropoulos et al., 1998 for laser impact).

2. *Shake-off*: If one electron is removed rapidly (sudden approximation) from an atom or a molecule, the wave function of the remaining electron has to be projected onto the new eigenstates of the altered potential. Parts of these states are in the continuum, so that a second electron can be "shaken off" in this relaxation process. This is known for example from beta decay, where the nuclear charge is changed. Shake-off is one of the mechanisms for double ionization by absorption or Compton scattering of a single photon.
3. *Two-step-one* (*TS1*): A simplified picture of TS1 is that one electron couples to the field and knocks out the second one via an electron–electron collision on its way through the atom (Samson, 1990). A close connection between the electron impact ionization cross section and the ratio of double to single ionization by single photon absorption as a function of the energy is seen experimentally (Samson, 1990) and theoretically (Kheifets, 2001), supporting this simple picture. For the TS1 mechanism the electron correlation is on a very short time scale (a few attoseconds) and confined to a small region of space (the size of the electron cloud).
4. *Rescattering*: Rescattering is a version of the TS1 mechanism which is induced only by a strong laser field. The mechanism was proposed originally by Kuchiev (1987) under the name "antenna model". He suggested that one of the electrons is driven in the laser field acting as an antenna absorbing the energy which it then shares with the other electron via correlation. Corkum (1993) and Schafer et al. (1993) extended this basic idea and interpreted the process in the two-step model: first one electron is set free by interaction with the field. Then it is accelerated by the laser field and is driven back to its parent ion with about 50% probability. Upon recollision with the ion the electron can recombine and emit higher harmonic radiation. Besides that it could be elastically scattered and further accelerated or it could be inelastically scattered with simultaneous excitation or ionization of the ion. In contrast to TS1 in this case there is a femtosecond time delay between the first and the second step. Also the wave function of the rescattered electron explores a larger region of space than in the case of TS1 (Watson et al., 1997; Lein et al., 2000, 2001).

These mechanism are shown in the Feynman diagrams in Fig. 3 (compare the discussion in Ken-ichi Hino et al. (1993); Kheifets (2001); McGuire (1997); Keller (2000) and Becker and Faisal (1996)). Here time

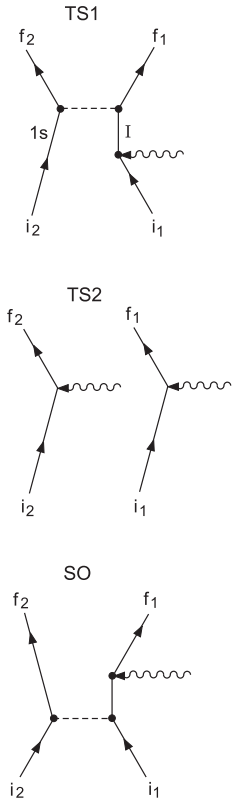

Fig. 3. Schematic Feynman diagrams for double ionization. The interaction with the photon field is shown by the snake line. For Compton scattering an outgoing photon has to be added. For single photon absorption and Compton scattering the two final states do not involve the field, for the strong field case the final states are field dressed states, e.g. Volkov states (see e.g. Becker and Faisal, 1996, 1999a, b, 2000).

progresses from bottom to top. The two electrons start out in a correlated initial state. The photon field couples once ore twice to one or two electrons. Compton scattering, i.e. an outgoing photon is not shown for simplicity. Note that TS1 and rescattering are represented by the same diagram (Becker and Faisal, 1996, 1999a, b, 2000). The difference is in the intermediate state denoted by I. In the strong field case a laser dressed state for example a Volkov state has to be used.

A helpful quantity in the discussion of mechanisms is the ratio R of doubly to singly charged ions produced. We denote R_γ, R_C and R_L for this ratio induced by photo absorption, Compton scattering or a strong field. Further we denote R_γ^∞ and R_C^∞ for the high photon energy limit of the respective ratios.

4. Double ionization by single photon absorption

In this chapter we discuss direct photo double ionization by single photon absorption. The closely related phenomenon of multiple ionization by two-step processes such as photoionization followed by single or multiple Auger decay will not be considered. Focus will be laid upon most fundamental two electron target system: the helium atom. Here two-step processes are impossible. This is a mature field now in which an impressive experimental and theoretical breakthrough has been achieved in the previous 10 years.

4.1. Energy, momentum and angular momentum considerations

Double ionization of helium by photo-absorption becomes possible if the energy of the photon is higher than the sum of the binding energies of both electrons ($E_{\text{ion}}^{2+} = 24.6\text{ eV} + 54.4\text{ eV} = 79\text{ eV}$). The excess energy $E_{\text{exc}} = E_\gamma - E_{\text{ion}}^{2+}$ can be shared among the two electrons in the continuum $E_1 + E_2 = E_{\text{exc}}$. The energy of the He^{2+} nucleus is negligible due to its heavy mass. In momentum space however the momenta of the electrons and the nucleus are of the same order of magnitude. From momentum conservation we obtain (assuming the atom at rest in the initial state):

$$k_\gamma = k_1 + k_2 + k_{He^{2+}}. \tag{2}$$

At non-relativistic energies the photon momentum can be neglected against the electron and ion momenta ($k_\gamma \approx 0$). Hence in the final state the sum of the two electron momenta is balanced by the ion. At photon energies of below typically 1 keV the dipole approximation is expected to hold. Therefore, the absorption of the photon leads to $\Delta L = 1$ and a change in parity between the initial and final state. Since the He ground state is an S state with gerade parity the three body final state is $^1P^o$. Angular momentum is not a good quantum number for the individual electron, but the two electrons have to couple to angular momentum 1 with odd parity. This $^1P^o$ character of the 3-body final state shapes the momentum and angular distributions as will be discussed below in more detail.

The criterion for the validity of the dipole approximation is $k_\gamma r \ll 1$, where r is the typical size of the system (e.g. 1 a.u.). For single ionization there are detailed calculations including higher order contributions Compton (1993), confirming the validity of the dipole approximation at $E_\gamma < 1$ keV. For double ionization no experimental evidence of any deviation from the dipole approximation have been found so far. Kornberg and Miraglia (1995) performed the only theoretical study of double ionization beyond the dipole approximation. They find no deviation for the ratio of double to single ionization cross section R_γ and only small deviation in the angular distribution at 1 keV. The further discussion in this chapter will therefore be restricted to phenomena and arguments within the dipole approximation.

The three particles in the final state are determined by 9 momentum components. Due to momentum and energy conservation however only 5 of them are linearly independent. The single photon double ionization process is therefore for given light polarization fully determined by a 5-fold differential cross section (FDCS). Sometimes this is also called a triply differential cross section. In this notion the linearly independent polar (ϑ) and azimuthal (Φ) angle of the electrons are combined to a solid angle (Ω), the fully differential cross section is then noted as $\mathrm{d}^3\sigma/\mathrm{d}E\,\mathrm{d}\Omega_1\,\mathrm{d}\Omega_2$. The dipole approximation results in a further symmetry axis in the final state (rotational symmetry around the polarization axis for linear light). This results in a further reduction to a four-fold differential cross section. To measure such a cross section the experimentalist can freely choose which 5 out of the 9 momentum components to measure. Using dispersive (Schwarzkopf et al., 1993, 1994; Schwarzkopf and Schmidt, 1995; Lablanquie et al., 1995; Dawson et al., 2001; Cvejanovic et al., 2000; Soejima et al., 1999), time-of-flight (Viefhaus et al., 1996a, b) electron spectrometers or advanced imaging techniques (Huetz and Mazeau, 2000) several groups succeeded in detecting the momenta of both electrons without detection of the ion. Alternatively COLTRIMS has been used to measure the momentum vector of the ion in coincidence with one of the electrons (Dörner et al., 1996b, 1998a; Bräuning et al., 1997, 1998; Mergel et al., 1998; Achler et al., 2001; Knapp et al., 2002a, b).

4.2. Probability and mechanism

The absolute value of R_γ is settled today to an accuracy of a few% experimentally and theoretically. R_γ rises almost linearly from threshold, reaches a maximum of 3.7% at $E_\gamma \approx 200$ eV and slowly approaches the high

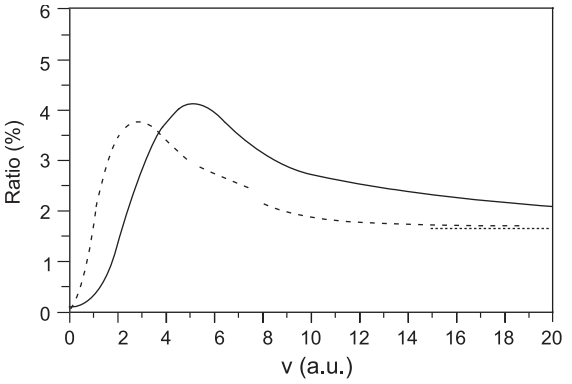

Fig. 4. Ratio of double to single ionization as a function of the velocity. Full line: sudden approximation; here v is the initial state velocity of the first electron (from Shi and Lin, 2002); dashed line low energy: experimental data for R_γ. Here v is taken to correspond to the excess energy above the double ionization threshold; dashed line high energy, CCC calculation for R_γ (Kheifets and Bray, 1998a), dotted line: high energy asymptote of 1.67% (figure from Shi and Lin, 2002).

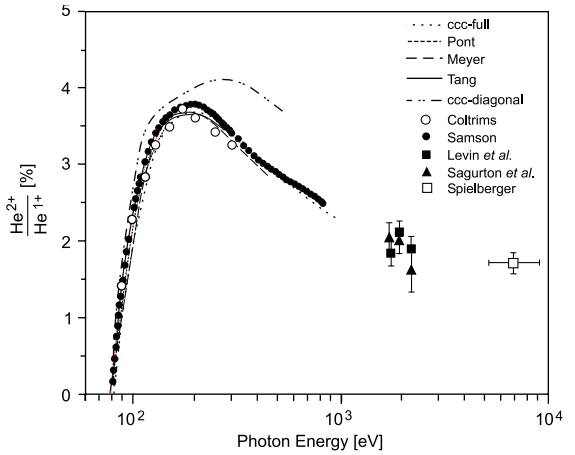

Fig. 5. Ratio of the total double to total single ionization cross section of Helium by photoabsorption. Open circles: COLTRIMS data (Dörner et al., 1996a), open square: COLTRIMS data for photoabsorption only (Spielberger et al., 1995), full dots Samson et al. (1998), full triangles (Sagurton et al., 1995), full square (Levin et al., 1996), dotted and dash dotted line (Kheifets, 2001), short dashed line (Pont and Shakeshaft, 1995a), long dashed line (Meyer et al., 1997), full line (Tang and Shimamura, 1995).

energy asymptotic value of 1.67% (Fig. 5). Below 1 keV the precision experiments by Dörner et al. (1996a) and Samson et al. (1998) are in good agreement with each other and supersede older experiments which were about 25% higher (see Dörner et al., 1996a for a comparison and discussion of these older experiments). In the high energy regime the pioneering work of Levin and coworkers reported an experimental value of $R_\gamma = 1.6 \pm 0.3\%$ at 2.8 keV of Levin et al. (1991). A measurement by Spielberger et al. (1995) at 7 keV found $R = 1.72 \pm 0.12\%$ and thus confirmed that the high energy limit has been reached. A collection of the data and some of the theoretical results are shown in Fig. 5.

The high energy value of R_γ is given by the shake-off process. As shown in Fig. 4 the shake-off probability depends on the velocity at which one picks the first electron from the initial state wavefunction. The high energy ratio for photoabsorption corresponds here to asymptotic high velocities. This asymptotic ratio thus probes the wavefunction for the case that one electron is infinitely fast. The shape of the curve in Fig. 5 from threshold to a few hundred eV can be understood in analogy to electron impact ionization. The rise at threshold like $E_{\mathrm{exc}}^{\alpha}$ with the Wannier coefficient $\alpha = 1.056$ is identical for double photoionization (Kossmann et al., 1988) and electron impact ionization (Samson, 1990). It is a consequence of final state phase space density and is described by the Wannier threshold law (Wannier, 1953).

4.3. Differential cross sections

Following the pioneering kinematically complete experiment on double photoionization of Helium by Schwarzkopf et al. (1993) today experimental data have been reported for energies from 0.1 eV (Huetz and Mazeau, 2000) to 450 eV above threshold (Knapp et al., 2002a) for linear and circular polarized light. This work together with the impressive theoretical progress in this field has recently be reviewed by Briggs and Schmidt (2000). We give here only a very brief overview. To discuss the main physical effects and the main features in the cross section, we start from partially differential data providing an overview progressing to fully differential data.

Fig. 6 shows the momentum distributions of one of the electrons, of the doubly charged ion and the Jakobi momentum $k_- = 1/2(k_1 - k_2)$ for 1, 20 and 100 eV above threshold. The second Jakobi momentum $k_+ = k_1 + k_2$ is opposite to the recoil ion momentum. The striking difference between the electronic and ionic distributions reflects part of the mechanisms leading to photo double ionization. The photon acts upon a charge dipole in the atom. This dipole might be thought of as consisting of the positive ion on one pole and either the center of charge of the electron pair or one of the electrons acting as the other pole. In either case the first step of the absorption of the photon will imprint the dipolar characteristics of the linear polarized photon on the distribution of the fragments of a charge dipole. The experiments indicate that the momentum distribution of the nucleus shows a memory of this absorption of the photon. At low excess energies this pattern is complete washed out in the electronic momentum distribution by

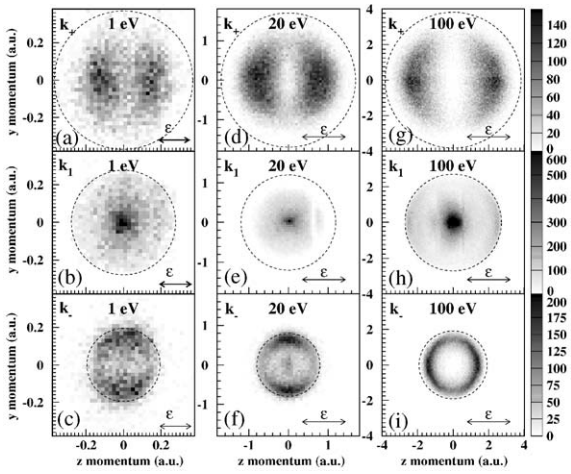

Fig. 6. Density plots of projections of the momentum distributions from double ionization of He by three different energies, from left to right: data sets for 1, 20 and 100 eV above threshold. The z and y components of the momentum are plotted on the horizontal and vertical axes, respectively. The polarization vector of the photon is in the z direction and the photon propagates in the x direction perpendicular to y and z. For the 100 eV above threshold measurement only events with $-1<k_x<1$. a.u. are projected onto the plane. (a), (d), (g) Momentum distribution of the He^{2+} ion (k_+) for 1, 20 and 100 eV above threshold. (b), (e), (h) electron momentum (k_1) and (c), (f), (i) electron pair relative momentum $(k_1-k_2)/2$. The circle locates the maximum possible momentum in each coordinate at the respective photon energy (from Dörner et al., 1996b; Bräuning et al., 1997; Knapp et al., 2002b).

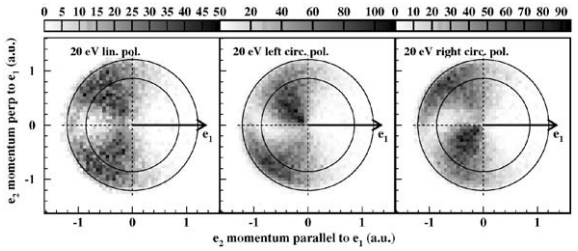

Fig. 7. Photo double ionization of He at 20 eV above threshold by linear, left and right circular polarized light. Shown is the momentum distribution of electron 2 for fixed direction of electron 1 as indicated by the arrow. There is no restriction on this momentum of electron 1. The plane of the figure is the momentum plane of the three particles. The data of (a) are integrated over all orientations of the polarization axis with respect to this plane. The figure samples the full cross sections, for all angular and energy distributions of the fragments. The outer circle corresponds to the maximum possible electron momentum, the inner one to the case of equal energy sharing. In (b) and (c) the light propagates into the plane of the figure, the electrons are confined to the plane perpendicular to the light propagation (from Dörner et al., 1998b and Achler et al., 2001).

the electron–electron interaction which is indispensable for double ionization. For 100 eV excess energy (and even more pronounced at 450 eV (Knapp et al., 2002a)) the fast electron also shows a dipolar emission pattern (Fig. 6(h)). It is very illustrative to switch from single electron coordinates $k_{1,2}$ to the Jakobi coordinates k_{+-}. This corresponds to a change to a molecule perspective of the He atom (Feagin and Briggs, 1986). This is most useful if the saddle region of the potential surface governs the final state of the reaction, which is expected close to threshold (Wannier, 1953). The two electrons create a two-center saddle potential in which in the nucleus is located. The coordinate k_- is aligned along the line connecting the two electrons and $-k_+$ is the momentum vector of the ionic core. At 1 and 20 eV there is a clear propensity for an escape of the nucleus perpendicular to k_-. This can be understood by a Wannier type analysis, which predicts, that double ionization near threshold can only be reached if ionic and electron motion are perpendicular, all other geometries lead to single ionization (Wannier, 1953; Huetz et al., 1991; Feagin, 1995, 1996; Kazanski and Ostrovsky, 1993, 1994, 1995). In the molecular picture the electronic separation $\vec{R}$ is interpreted as a molecular axis and the projection m of the total angular momentum on this axis is taken as an approximate quantum number. This propensity for $m=1$ breaks down at 100 eV. Without this propensity the main motivation for analyzing the process in Jacobi coordinates is lost. The evolution of the three-body system is no longer governed by the saddle region of the potential.

We now investigate the internal structure of the two electron continuum in k_1,k_2 coordinates (Fig. 7). Neglecting the (small) photon momentum the vector momenta of ion and both electrons have to be in one plane. Fig. 7(a) shows the electron momentum distribution in this plane for linear polarized light. The data are integrated over all orientations of the polarization axis with respect to this plane, the horizontal axis is chosen to be the direction of one electron. The structure of the observed momentum distribution is dominated by two physical effects. First the electron–electron repulsion leads to almost no intensity for both electrons in the same half plane. Second, the $^1P^o$ symmetry leads to a node in the square of the wave function at the point $\mathbf{k}_1=-\mathbf{k}_2$ (Schwarzkopf et al., 1993; Huetz et al., 1991; Maulbetsch and Briggs, 1995; Malegat et al., 1997). The corresponding data for left and right circular polarized light are shown in Fig. 7(b) and (c). They show a strong circular dichroism, i.e. a dependence on the chirality of the light. This might be surprising since the helium atom is perfectly spherical symmetric. Berakdar and Klar (1992) first pointed out that for circular dichroism to occur it is sufficient that the direction of light propagation and the momentum vectors of the electrons span a tripod of defined handedness. This is the case if the two electrons and the light direction are non coplanar and

the two electrons have unequal energy (see Berakdar et al., 1993; Berakdar, 1998, 1999; Berakdar and Klar, 2001) for a detailed discussion and experimental results (Soejima et al., 1999; Viefhaus et al., 1996a; Mergel et al., 1998; Achler et al., 2001; Kheifets et al., 1999; Kheifets and Bray, 1998b; Collins et al., 2002).

Finally fully differential cross section can be investigated. The main features seen here at low to moderate excess energies is the interplay between selection rules resulting from the $^1P^o$ symmetry and the electron repulsion. A detailed discussion goes beyond the scope of the present review, we refer the reader to (Briggs and Schmidt, 2000). In general very good agreement is found between the experimental data even on absolute scale and the most advanced theoretical approaches (Kheifets and Bray, 1998b, c, 2000; Malegat et al., 2000, 2002; Selles et al., 2002; Pont and Shakeshaft, 1995b, 1996; Colgan et al., 2001; Colgan and Pindzola, 2002). At very high excess energies (450 eV (Knapp et al., 2002a) finally one electron is found to leave fast, carrying away most of the photon energy and angular momentum. In the angular distributions of the second slow electron clear traces of mechanism which lead to its ejection can be found (see also Keller, 2000; Teng and Shakeshaft, 1994). Electrons emitted via the shake-off mechanism are expected to be isotropic or slightly backward directed with respect to the primary electron, while electrons knocked out in a binary collision (TS1-mechanism) will yield 90° between the two electrons. At 529 eV photon energy the electron angular distributions show a dominance of the shake-off mechanism for secondary electrons which have very low energy (2 eV) and display clear evidence that an inelastic electron–electron scattering is necessary to produce secondary electrons of 30 eV (Knapp et al., 2002a) (see Fig. 8).

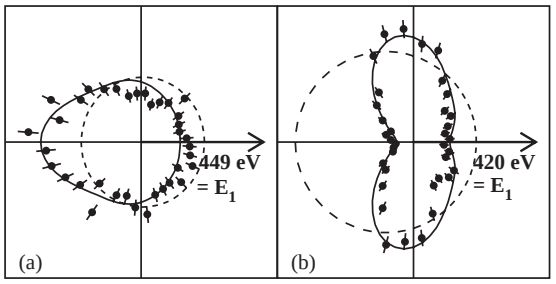

Fig. 8. Fully differential cross section of the He photo double ionization at 529 eV photon energy. The primary photo electron 1 indicated by the arrow, the polarization is horizontal, the angular distribution of the complementary electron 2 with energy E_2 given by the symbols. (a) $447 < E_1 < 450$ eV, $0 < E_2 < 3$ eV, (b) $410 < E_1 < 430$ eV, $20 < E_2 < 40$ eV. (a) shows the dominance of shake-off, the 90° emission in (b) indicates the importance of TS1 at this energy. The solid line shows the full CCC calculation, the dashed line is the shake-off only part of the CCC calculation (from Knapp et al., 2002a).

Such connection between the fully differential cross section and the mechanisms discussed in Section 3 can only be found at high photon energies. The main reason is that the experimental identification of mechanisms requires a signature for which electron primarily absorbed the photon. At low photon energy there is no answer to this question, since momentum, energy and angular momentum exchange between the two electrons after the photon is absorbed masking the first step completely. Therefore at low photon energies the assignment of mechanisms is based on theory and the energy dependence of the cross section ratio only (Fig. 5).

5. Double ionisation by Compton scattering

At photon energies above 6 keV, the ionization cross section of helium by Compton scattering exceeds the photo-absorption cross section (Bergstrom et al., 1995; Samson et al., 1993) (see Fig. 9).

To experimentally determine the ratio of the total double to total single ionization cross section it is therefore necessary to detect not only the charge state of the ions, but also determine whether they are created by absorption or Compton scattering. This can be done most easily by measuring the ion momentum. As shown in Fig. 1 ions from photo-absorption compensate the electron momenta and hence have comparably high momenta, while Compton scattering produces cold ions. This clear distinction is obscured only at extremely high photon energies, where a new double ionization mechanism by absorbtion is predicted (Drukarev, 1995; Ya Amusia et al., 2002). This so far unobserved mechanism leads to two almost equal energy electron compensating their momenta and leaving a very slow ion behind. The cross section for this process, however is negligible compared to Compton scattering.

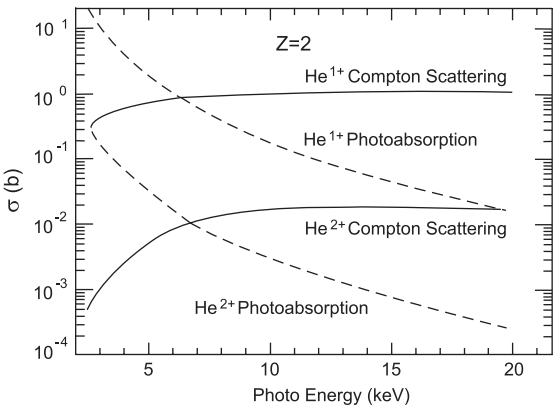

Fig. 9. Calculated total cross section for single and double ionization of Helium by photoabsorption and Compton scattering (from Bergstrom et al., 1995).

This has been used by Samson and coworkers to measure the single ionization Compton scattering cross section (Samson et al., 1994). Spielberger and coworkers pioneered COLTRIMS to measure R_γ and R_C (Spielberger et al., 1995) separately (see also Spielberger et al., 1996, 1999; Krässig et al., 1999). The best values for the photon energy dependence of the ratio by Compton scattering is shown in Fig. 10. For high photon energies the ratio approaches a constant. The theoretical high energy limit is given purely by the shake-off process to be 0.84% for Compton scattering. This is significantly different from the value of $R_\gamma^\infty = 1.66\%$. The physical reason for this difference is that photo absorption and Compton scattering sample a different part of the first electrons initial state distribution (see Table 1). Photo-absorption samples high momenta in the initial state or in the coordinate representation removes one electron from close to the nucleus. Compton scattering at high photon energies in contrast is not sensitive on the electrons initial momentum or position. Therefore Compton scattering samples the full initial state and hence the asymptotic ratio by Compton scattering of 0.84% is a weighted average over the full line in Fig. 4 where the weight for each velocity is given by the probability to find the respective electron velocity in the initial state. This argument assumes the sudden approximation to be valid (Åberg, 1970, 1976), i.e. the first electron to be removed instantaneously. Compton scattering always leads to a distribution of electron energies. Spielberger et al. (1999) have shown that even at photon energies of 100 keV the experimental value for the ratio is still slightly above the asymptotic value (see Fig. 10). In their theoretical analysis they could show that this can be partially explained by the fraction of low energetic primary electrons contributing at these photon energies. Their final state interaction leads to a slightly increase of the ratio above the sudden approximation value.

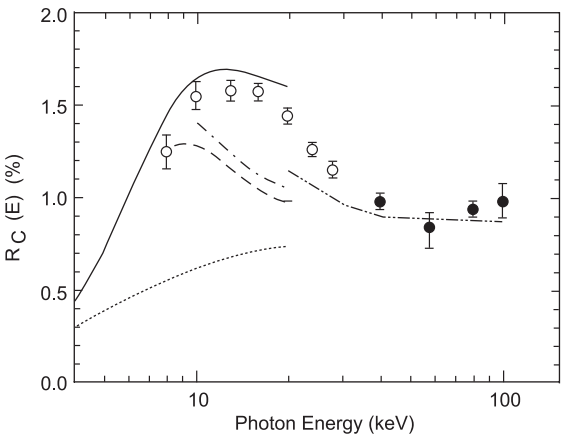

Fig. 10. Ratio of double to single ionization by Compton scattering. Open circles: COLTRIMS experiment from (Krässig et al., 1999), full circles: COLTRIMS experiment from Spielberger et al. (1999) and Spielberger et al. (1996). Theory: solid curve Many Body perturbation theory (Bergstrom et al., 1995), dashed curve 3C final state (Andersson and Burgdörfer, 1994), dot dashed CI final state (Andersson and Burgdörfer, 1994), dot dot dashed curve 3C final state (Spielberger et al., 1999), dotted curve (Surić et al., 1994) (from (Krässig et al., 1999)).

Double ionization by Compton scattering is today still a major experimental challenge. Only ratios of total cross sections have been measured. No differential experimental data are available. In principle 8 degrees of freedom would have to be determined for a fully differential cross section. Such data are very desirable for the future since they complement (e,3e) and ion impact double ionization studies but avoid some of the problems since there are only 3 charged particles in the final state.

6. Strong field double ionization

6.1. Sequential versus nonsequential double ionization

Single photon absorption and Compton scattering both depend linear on the photon intensity. In both cases double ionization is always a result of electron–electron correlation. In the strong field, long wavelength

Table 1
Some key properties of different types of light-matter interactions

	Photo absorption	Compton scattering	Strong field
Energy conservation	$E_e = E_\gamma - E_{bind} - E_{exc}$	$E_e = E_\gamma$–-$E_{\gamma'} - E_{bind}$	
Momenta	$k_e \approx -k_{ion}$	$k_e \approx -(k_\gamma - k'_\gamma)$	$k_e \approx -k_{ion}$
Role of Ion	Balance k_e	Spectator	Balance k_e
Main source of k_e	Initial state	Photon	Field acceleration
Main source of k_{ion}	Initial state	Initial state	Field acceleration
Angular momentum	$\Delta L = 1$ dominant at low energies	High ΔL	ΔL up to number of absorbed photons
Intensity dependence	Linear	Linear	Highly nonlinear
Double ionization via	Shake-off, TS1	Shake-off, TS1	TS2, rescattering

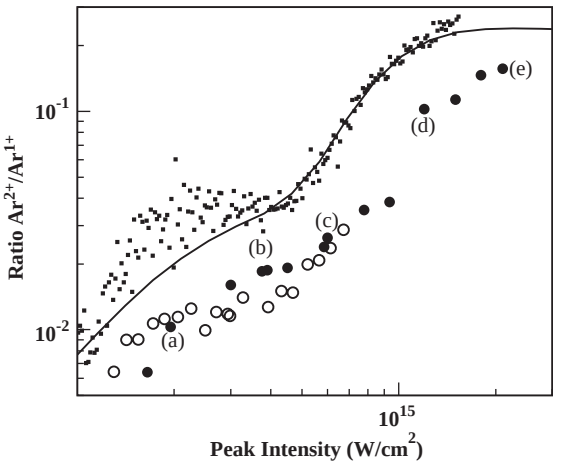

Fig. 11. Ratio of double to single ionization of Argon as a function of the peak intensity at 800 nm. The steep rise at 4.5×10^{14} W/cm^2 is due to the onset of sequential ionization. The full line shows an S-matrix calculation by Becker and Faisal (1999b). Small dots: from Larochelle et al. (1998), open circles: from Guo et al. (1998), large full circles: (Weber et al., 2000a) (figure from (Weber et al., 2000a)).

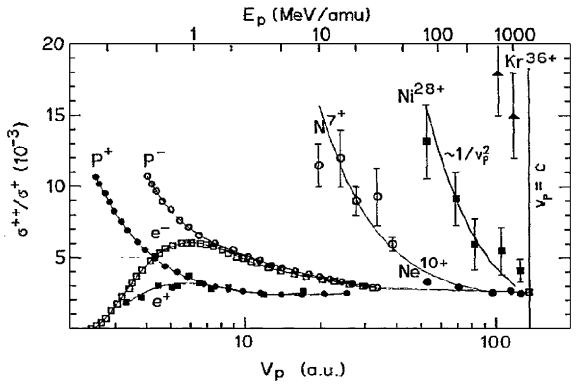

Fig. 12. Ratio of double to single ionization by charged particle impact as a function of the projectile velocity. The projectile charge state is given in the figure. The perturbation falls with rising velocity, i.e. the x-axis is inverse to the one in Fig. 11 (from Ullrich et al., 1993).

case in contrast it is always necessary to absorb many photon to achieve ionization. Therefore an additional double ionization mechanism of TS2 or sequential ionization (in the sense of two sequential interaction with the photon field, one for each electron) becomes possible. This process does not require any electron correlation. The sequential (TS2) and nonsequential (TS1 or shake-off) process have very different dependence on the photon intensity, or perturbation. The processes can be most easily distinguished by considering the ratio of double to single ionization as function of field strength: for nonsequential ionization the removal of the second electron does not require an additional interaction with the field and hence the ratio should be intensity independent, for the sequential double ionization it will rise with the intensity. This is shown in Fig. 11 for double ionization of Argon at 800 nm. Above 4.5×10^{14} W/cm^2 there is a steep rise due to the onset of the TS2 process. Long before such behavior was rediscovered in the field of laser atom interaction a very similar phenomenon was seen in ion atom collision physics (McGuire, 1997; Ullrich et al., 1993; Knudsen et al., 1984; Andersen et al., 1986, 1987, 1989). Here the field causing the ionization is not an optical field but the field of an ion flying by. The perturbation scales with q/v the projectile charge over its velocity. A compilation of the results for different charge state projectiles is shown in Fig. 12. For each charge state projectile there is a lower limit velocity below which the ratio starts to rise due to the onset of the TS2 process (sequential ionization).

6.2. *Mechanisms for nonsequential double ionization*

At intermediate laser intensities the double ionization yield exceeds the yield expected by the sequential ionization mechanism (Fittinghoff et al., 1992; Walker et al., 1994) by several orders of magnitude. Originally it had been speculated that shake-off might be responsible for this enhancement. From the arguments given above this can be ruled out. Contrary to high energy single photon absorption, the laser field removes the first electron extremely softly from far away from the nucleus and from the small momentum part of the initial state wave function. Consequently residual ion has much time to adapt to this slow change adiabatically. Hence shake-off will be negligible. This has been also confirmed by calculation of the shake-off diagram (Becker and Faisal, 2002).

It is consensus today that the rescattering process in some form is responsible for the high double ionization rate observed in the experiments. A strong experimental evidence for the rescattering and against the shake-off mechanism in strong fields provided was already early on by the observation that double ejection is strongly suppressed in ionization with circularly polarized light (Fittinghoff et al., 1994; Dietrich et al., 1994) (and Figure 19 in DiMauro and Agostini (1995)). The rescattering mechanism is inhibited by the circular polarization since the rotating electric field does not drive the electrons back to their origin. The other mechanisms, in contrast, are expected to be polarization independent.

To gain further insight in the double ionization process clearly differential measurements beyond the ion yield are necessary. Two types of such experiments have been reported recently: Electron time-of-flight measurements in coincidence with the ion charge state

(Witzel et al., 2000; Lafon et al., 2001) and those using COLTRIMS, where at first only the ion momenta (Weber et al., 2000b, 2001a; Moshammer et al., 2000) and later the ion momenta in coincidence with one electron (Weber et al., 2000c; Weckenbrock et al., 2001; Weckenbrock, 2001; Feuerstein et al., 2001) have been measured.

In the following sections we discuss the measured momenta of the doubly charged ions (Section 6.3) and the correlated electron momenta (Section 6.4).

6.3. Ion momenta

The momentum distributions of doubly charged He (Weber et al., 2000b), Neon (Moshammer et al., 2000), and Argon (Weber et al., 2000a) ions in the intensity regime where nonsequential ionization is expected to be dominant have been found to be very different from those of the singly charged. They exhibit a pronounced double peak structure. The results for Neon are shown in Fig. 13. This double peak structure is a direct consequence of the time delay between the removal of the first electron and the knock out of the second one in the rescattering process as we will discuss below. Consequently this double peak structure disappears at high intensities where the sequential double ionization dominates (Fig. 13 inset (3)). In this sequential regime the momentum distribution of the doubly charged ions can be simulated by a convolution of the singly charged ion momentum distribution with itself (Weber et al., 2000a), as it can be expected for an independent two-step process.

What is the physical origin of the double peak structure? Analogous to the situation for single ionization discussed above (Eq. (1)) one can estimate the net momentum accumulated by the doubly charged ion from the laser pulse as

$$p_z^{\mathrm{He}^{2+}}(t_\infty) = \int_{t_1}^{t_{12}} E(t)\sin(\omega t)\,\mathrm{d}t + 2\int_{t_{12}}^{t_\infty} E(t)\sin(\omega t)\,\mathrm{d}t. \quad (3)$$

The first electron is removed at time t_1 and the ion switches its charge from 1^+ to 2^+ at time t_{12}. It is assumed that there is no momentum transfer to the ion from the first emitted electron during double ionization. Thus, as in the case of single ionization the phase of the field at the instant of the emission of the first and of the second electron is encoded in the ion momentum.

Shake-off and TS2 will both lead to a momentum distribution peaking at zero, similar to single ionization. In both cases the emission of the second electron follows the first with a time delay, which is orders of magnitude shorter than the laser period. Hence $t_{12} = t_1$ in Eq. (3) and since the first electron is emitted most likely at the field maximum $p_z^{\mathrm{He}^{2+}}$ would also peak at zero for shake-off and TS1. Consequently, the observed double peak structure for He and Ne directly rules out these mechanisms.

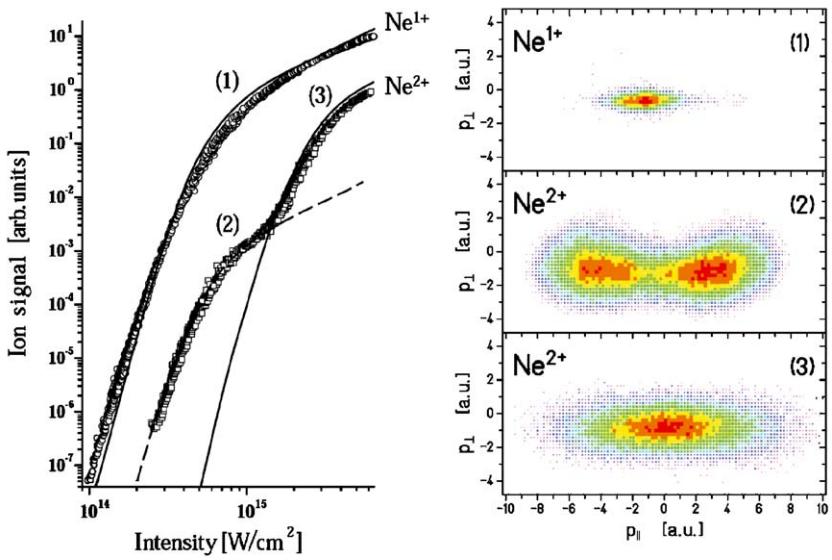

Fig. 13. Neon double ionization by 800 nm, 25 fs laser pulses. Left panel: Rate of single and double ionization as a function of the laser power (from Larochelle et al., 1998). The full line shows the rate calculated in an independent event model. Right panel: Recoil ion momentum distributions at intensities marked in the left panel. Horizontal axis: Momentum component parallel to the electric field. Vertical axis: One momentum component perpendicular to the field (data partially from Moshammer et al., 2001).

For the rescattering there is a significant time delay between the emission of the first electron and the return to its parent ion. Estimating t_{12} for a rescattering trajectory which has sufficient energy to ionize leads to ion momenta close to the measured peak positions (Weber et al., 2000b; Moshammer et al., 2000; Feuerstein et al., 2000). The high momenta of the doubly and triply charged ions are a direct proof of the time delay introduced by the rescattering trajectory. It is this time delay with respect to the field maximum, which is responsible for multiple ionization and allows an effective net momentum transfer to the ion by accelerating the parent ion. Within the classical rescattering model the final momentum of the doubly charged ion will be the momentum received from the field (as given by Eq. (3)) plus the momentum transfer from the recolliding electron to the ion.

The experiments spawned a variety of different theoretical investigations of this problem. Becker and Faisal (2000) have evaluated the diagram for TS1 adapted to the laser field situation shown in Fig. 3. They could show that only the inclusion of the laser electron interaction in the form of Volkov states for the two outgoing electrons yields the observed double peak (see also Kopold et al., 2000; Goreslavskii and Popruzhenko, 2001a, b). Classical trajectory Monte Carlo Calculations (Chen et al., 2000), Wannier type calculations (Sacha and Eckhardt, 2001) and direct solutions of the one dimensional Schrödinger equation (Lein et al., 2000) also could reproduce the double peak structure and supported the physical interpretation given above. However in most cases the agreement with the experiment was qualitative and many questions on the details of the process are still open. We will give a brief account of these question following the next section.

6.4. Correlated electron momenta

More information can be obtained from the momentum correlation between the two electrons. Up to present, however, no fully differential experiment has been reported for multiphoton double ionization. Weber et al. (2000c) and Feuerstein et al. (2001) reported measurements observing only the momentum component parallel to the field of electron and ion integrating over all other momentum components. Weckenbrock et al. (2001) and Moshammer et al. (2001) have detected the transverse momentum of one of the electrons in addition to the parallel momenta. In these experiments, however, the transverse momentum of the ion could not be measured with sufficient resolution, mainly due to the internal temperature of the gas-jet for argon and neon targets. Experiments on helium have not yet been reported but are in preparation in several laboratories.

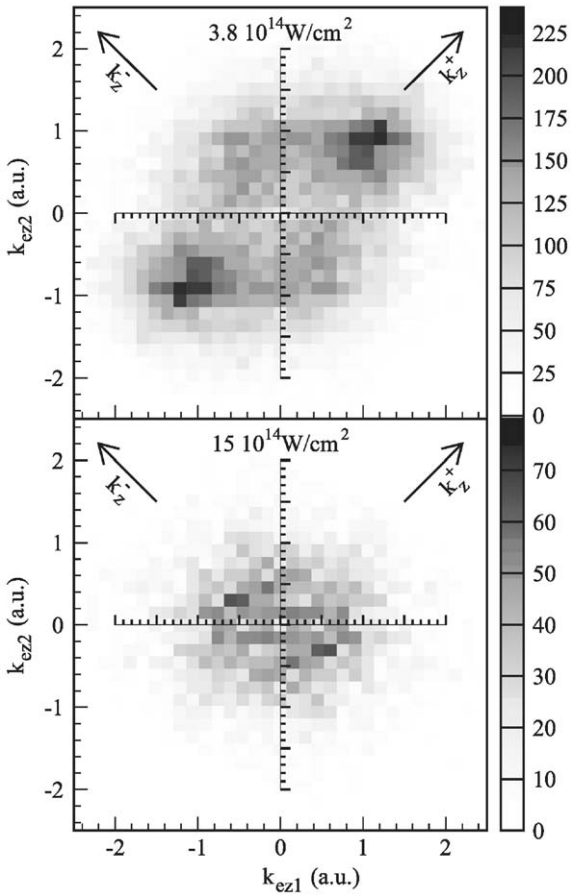

Fig. 14. Momentum correlation between the two emitted electrons when an Ar^{2+} ion is produced in the focus of a 220 fs, 800 nm laser pulse at peak intensities of 3.8×10^{14} and 15×10^{14} W/cm^2. The horizontal axis shows the momentum component of one electron along the polarization of the laser field; the vertical axis represents the same momentum component of the corresponding second electron. Same sign of the momenta for both electrons represents an emission to the same half sphere. The data are integrated over the momentum components in the direction perpendicular to the polarization direction. The gray shading shows the differential rate in arbitrary units on a linear scale (adapted from (Weber et al., 2000c)). Compare also to (Feuerstein et al., 2001).

The correlation between the momentum components parallel to the polarization is shown in Fig. 14. The electron momenta are integrated over all momentum components perpendicular to the field direction. Events in the first and third quadrant are those where both electrons are emitted to the same hemisphere, the second and fourth quadrant correspond to emission to opposite hemispheres. The upper panel shows the electron momenta at an intensity of 3.6×10^{14} W/cm^2, which is in the regime where nonsequential ionization is

expected. The distribution shows a strong correlation between the two electrons, they are most likely emitted to the same hemisphere with a similar momentum of about 1 au. At higher intensity, where double ionization proceeds sequentially this correlation is lost (lower panel in Fig. 14).

To interpret the correlation pattern it is helpful to consider the relationship between the electron and the recoil ion momenta. The momenta $k_z^+ = k_{ez1} + k_{ez2}$ and $k_z^- = k_{ez1} - k_{ez2}$ with $k_{z\mathrm{ion}} = -k_z^+$ are along the diagonals of Fig. 14. Hence the recoil ion momentum distribution is simply a projection of Fig. 14 onto the diagonal k_z^+. The coordinates k_z^+ and k_z^- are helpful to illustrate the relative importance of the two counteracting effects of electron–electron repulsion and acceleration of particles by the optical field. Both influence the final state momenta in different ways. Electron repulsion (and two-body electron–electron scattering) does not change k_z^+ but contributes to the momentum k_z^-. On the other hand, once both electrons are set free, the momentum transfer received from the field is identical for both. Therefore, this part of the acceleration does not change k_z^- but adds to k_z^+. The observed wide k_z^+ and narrow k_z^- distributions thus indicate that the joint acceleration of the electrons in the laser field clearly dominates over the influence of electron repulsion. Similar data for the single photon case can be found in Weber et al. (2001b).

For Ar double ionization Weckenbrock et al. (2001) and Moshammer et al. (2002) measured in addition to the momentum parallel to the field also the transverse momentum of the detected electron. Both find that the correlation pattern strongly depends on this transverse momentum. If one electron is emitted with any transverse momentum larger than 0.1 au (i.e. with some angle to the polarization axis) one mostly finds both electrons with a similar momentum component in the field direction. It is this configuration which dominates the integrated spectrum in Fig. 14. If, however, one electron is emitted parallel to the polarization with a very small transverse momentum window of $p_\perp < 0.1$ au one finds that the parallel momentum distribution does no longer peak on the diagonal. In this case most likely one electron is fast and the other slow. This might be due to the fact that the $1/r_{12}$ potential forces the electrons into different regions in the three dimensional phase space. Consequently, for electrons to have equal parallel momentum some angle between them is required. Accordingly, the peak at $p_{ez1} = p_{ez2} = 1$ au is found to be most pronounced if at least one of the electrons has considerable transverse momentum (see Goreslavskii and Popruzhenko, 2001a; Goreslavskii et al., 2001). Even so there are no fully differential data in this field available today one can already conclude that in the strong field case the mean angle between the two electrons will be much smaller than 90°. This is in contrast to the single photon case (see Fig. 7). This apparent suppression of the influence of final state electron repulsion is solely a consequence of the constant linear drift momentum along the polarization which is added by the laser field after both electrons are in the continuum.

7. Summary and open questions

Double ionization by one and many photons is a fascinating direct observation window for many-particle correlation effects. The field was driven by a very fruitful interplay of theory and experiment. From the subfields of double ionization by single photon absorption, Compton scattering and strong field multi photon absorption clearly the first one is most mature today. Even absolute and fully differential cross sections are widely understood for the single photon case. The ionization mechanisms here are TS1 at low energies and shake-off at high energies. In the differential cross section up to at least 100 eV the final state momentum distribution is not determined by the double escape mechanism but by a subtle interplay of electron repulsion and selection rules resulting from the symmetry and angular momentum ($^1P^o$ for He) of the final state.

The encouraging progress in our understanding of single photon double ionization points already to the next challenge: single photon direct double ionization of solids (Berakdar et al., 1998) and small molecules. Double ionization of the H_2 molecule has already been studied on the level of partial differential cross sections (Kossmann et al., 1989; Reddish et al., 1997; Wightman et al., 1998; Reddish and Feagin, 1998; Scherer et al., 1998; Dörner et al., 1998c) and kinematically complete experiment are underway (Weber, 2003).

For Compton scattering differential data still remain a major challenge for theory and experiment. One of the reasons why this is of particular interest, is that there are almost no selection rules determining the final state. It can therefore be hoped that the more interesting effect like the real quantum dynamics of a three body system and possibly fingerprints of the initial state will not be masked by strong but well understood effects of selection rules.

For the case of double ionization in strong laser fields much progress has been made in the recent 3 years. The rescattering has been clearly proven as the mechanism at an intermediate range of intensities. The details of the rescattering process however are still heavily discussed: what is the role of exited intermediate states and at which time is the energy absorbed from the field, what is the momentum exchange perpendicular to the field, what is the mechanism for subcritical fields? Fully differential data for He are the goal of intensive work at

many laboratories. It might seem surprising but it is characteristic for the fragmentariness of our understanding, that the quantum nature of the field and the selection rules which dominate the single photon case have not even been discussed for the multiphoton case (see Becker and Faisal, 1994 for one exemption).

Clearly there is a huge gap between single photon double ionization with synchrotron radiation and double ionization by 800 nm femto second laser light, where more than 53 photon (1.5 eV) have to be absorbed to achieve double ionization of Helium. With the advent free electron lasers in the VUV like the TESLA test facility and later on TESLA at DESY in Hamburg in the near future this gap will be closed from the experimental side.

Acknowledgements

This work is supported by DFG, BMBF, GSI. We thank our colleagues C.L. Cocke, M.H. Prior, A. Landers, H. Bräuning, L. Spielberger, B. Krässig, A. Kheifets, J. Berakdar, S. Keller, A. Becker, J. McGuire, J. Ullrich and R. Moshammer for long standing collaboration on the subject discussed here.

References

Åberg, T., 1970. Phys. Rev. A 2, 1726.
Åberg, T., 1976. In: Wuilleumier, F.J. (Ed.), Photoionization and other Probes of Many-Electron Interactions, S. 49. Plenum Press, New York.
Achler, M., Mergel, V., Spielberger, L., Azuma, Y., Dörner, R., Schmidt-Böcking, H., 2001. J. Phys. B 34, L965.
Andersson, L.R., Burgdörfer, J., 1994. Phys. Rev. A 50, R2810.
Andersen, L.H., Hvelplund, P., Knudsen, H., Moller, S.P., Elsener, K., Rensfelt, K.-G., Uggerhoj, E., 1986. Phys. Rev. Lett. 57, 2147.
Andersen, L.H., Hvelplund, P., Knudsen, H., Moller, S.P., Sorensen, A.H., Elsener, K., Rensfelt, K.-G., Uggerhoj, E., 1987. Phys. Rev. A 36, 3612.
Andersen, L.H., Hvelplund, P., Knudsen, H., Moller, S.P., Pedersen, J.O.P., Tang-Pedersen, S., Uggerhoj, E., Elsener, K., Morenzoni, E., 1989. Phys. Rev. A 40, 7366.
Becker, A., Faisal, F.H.M., 1994. Phys. Rev. A 50, 3256.
Becker, A., Faisal, F.H.M., 1996. J. Phys. B 29, L197.
Becker, A., Faisal, F.H.M., 1999a. Phys. Rev. A 59, R1742.
Becker, A., Faisal, F.H.M., 1999b. J. Phys. B 32, L335.
Becker, A., Faisal, F.H.M., 2000. Phys. Rev. Lett. 84, 3546.
Becker, A., Faisal, F.H.M., 2002. Phys. Rev. Lett. 89, 193003.
Berakdar, J., 1998. J. Phys. B 31, 3167.
Berakdar, J., 1999. J. Phys. B 32, L25.
Berakdar, J., Klar, H., 1992. Phys. Rev. Lett. 69, 1175.
Berakdar, J., Klar, H., 2001. Phys. Rep. 340, 474.
Berakdar, J., Klar, H., Huetz, A., Selles, P., 1993. J. Phys. B 26, 1463.
Berakdar, J., Samarin, S.N., Herrmann, R., Kirschner, J., 1998. Phys. Rev. Lett. 81, 3535.
Bergstrom Jr., P.M., Hino, K., Macek, J., 1995. Phys. Rev. A 51, 3044.
Bräuning, H.P., Dörner, R., Cocke, C.L., Prior, M.H., Krässig, B., Bräuning-Demian, A., Carnes, K., Dreuil, S., Mergel, V., Richard, P., Ullrich, J., Schmidt-Böcking, H., 1997. J. Phys. B 30, L649.
Bräuning, H.P., Dörner, R., Cocke, C.L., Prior, M.H., Krässig, B., Kheifets, A., Bray, I., Bräuning-Demian, A., Carnes, K., Dreuil, S., Mergel, V., Richard, P., Ullrich, J., Schmidt-Böcking, H., 1998. J. Phys. B 31, 5149.
Briggs, J., Schmidt, V., 2000. J. Phys. 33, R1.
Chen, J., Liu, J., Fu, L.B., Zheng, W.M., 2000. Phys. Rev. 63, 011404R.
Colgan, J., Pindzola, M.S., 2002. Phys. Rev. A 65, 032729.
Colgan, J., Pindzola, M.S., Robicheaux, F., 2001. J. Phys. 34, L457.
Collins, S.A., Cvejanovic, S., Dawson, C., Reddish, T., Seccombe, D.P., Huetz, A., Malegat, L., Selles, P., Kazansky, A.K., Danjo, A., Soejima, K., Okuno, K., Yagishita, A., 2002. Phys. Rev. A 65, 052717.
Compton, J.W., 1993. Phys. Rev. A 47, 1841.
Corkum, P.B., 1993. Phys. Rev. Lett. 71, 1994.
Cvejanovic, S., Wightman, J.P., Reddish, T.J., Maulbetsch, F., MacDonald, M.A., Kheifets, A.S., Bray, I., 2000. J. Phys. B 33, 265.
Dawson, C., Cvejanovic, S., Seccombe, D.P., Reddish, T.J., Maulbetsch, F., Huetz, A., Mazeau, J., Kheifets, A.S., 2001. J. Phys. B 34, L525.
Dietrich, P., Burnett, N.H., Ivanov, M., Corkum, P.B., 1994. Phys. Rev. A 50, R3585.
DiMauro, L.F., Agostini, P., 1995. Advances in Atomic and Molecular Physics. Academic Press, New York.
Dörner, R., Vogt, T., Mergel, V., Khemliche, H., Kravis, S., Cocke, C.L., Ullrich, J., Unverzagt, M., Spielberger, L., Damrau, M., Jagutzki, O., Ali, I., Weaver, B., Ullmann, K., Hsu, C.C., Jung, M., Kanter, E.P., Sonntag, B., Prior, M.H., Rotenberg, E., Denlinger, J., Warwick, T., Manson, S.T., Schmidt-Böcking, H., 1996a. Phys. Rev. Lett. 76, 2654.
Dörner, R., Feagin, J., Cocke, C.L., Bräuning, H., Jagutzki, O., Jung, M., Kanter, E.P., Khemliche, H., Kravis, S., Mergel, V., Prior, M.H., Schmidt-Böcking, H., Spielberger, L., Ullrich, J., Unverzagt, M., Vogt, T., 1996b. Phys. Rev. Lett. 77, 1024, see also erratum in 1997. Phys. Rev. Lett. 78, 2031.
Dörner, R., Bräuning, H., Feagin, J.M., Mergel, V., Jagutzki, O., Spielberger, L., Vogt, T., Khemliche, H., Prior, M.H., Ullrich, J., Cocke, C.L., Schmidt-Böcking, H., 1998a. Phys. Rev. A 57, 1074.
Dörner, R., Mergel, V., Bräuning, H., Achler, M., Weber, T., Khayyat, Kh., Jagutzki, O., Spielberger, L., Ullrich, J., Moshammer, R., Azuma, Y., Prior, M.H., Cocke, C.L., Schmidt-Böcking, H., 1998b. In: Oks, E., Pindzola, M. (Eds.), Atomic Processes in Plasmas, AIP Conference Proceedings, Vol. 443, American Institute of Physics, Woodbury, New York.
Dörner, R., Bräuning, H., Jagutzki, O., Mergel, V., Achler, M., Moshammer, R., Feagin, J., Bräuning-Demian, A., Spielberger, L., McGuire, J.H., Prior, M.H., Berrah, N., Bozek, J., Cocke, C.L., Schmidt-Böcking, H., 1998c. Phys. Rev. Lett. 81, 5776.

Dörner, R., Weber, Th., Weckenbrock, M., Staudte, A., Hattass, M., Schmidt-Böcking, H., Moshammer, R., Ullrich, J., 2002. Adv. At. Mol. Opt. Phys. 48, 1.
Drukarev, E.G., 1995. Phys. Rev. A 51, R2684.
Feagin, J.M., 1995. J. Phys. B 28, 1495.
Feagin, J.M., 1996. J. Phys. B 29, l551.
Feagin, J.M., Briggs, J.S., 1986. Phys. Rev. Lett. 57, 984.
Feuerstein, B., Moshammer, R., Ullrich, J., 2000. J. Phys. B 33, L823.
Feuerstein, B., Moshammer, R., Fischer, D., Dorn, A., Schröter, C.D., Deipenwisch, J., Lopez-Urrutia, J.R.C., Höhr, C., Neumayer, P., Ullrich, J., Rottke, H., Trump, C., Wittmann, M., Korn, G., Sandner, W., 2001. Phys. Rev. Lett. 87, 043003.
Fittinghoff, D.N., Bolton, P.R., Chang, B., Kulander, K.D., 1992. Phys. Rev. Lett. 69, 2642.
Fittinghoff, D.N., Bolton, P.R., Chang, B., Kulander, K.D., 1994. Phys. Rev. A 49, 2174.
Goreslavskii, S.P., Popruzhenko, S.V., 2001a. Opt. Express 8, 395. http://www.opticsexpress.org/oearchive/source/30694.htm.
Goreslavskii, S.P., Popruzhenko, S.V., 2001b. J. Phys. B 34, L239.
Goreslavskii, S.P., Popruzhenko, S.V., Kopold, R., Becker, W., 2001. Phys. Rev. 64, 053402.
Guo, C., Li, M., Nibarger, J.P., Gibson, G.N., 1998. Phys. Rev. A 58, R4271.
Huetz, A., Mazeau, J., 2000. Phys. Rev. Lett. 85, 530.
Huetz, A., Selles, P., Waymel, D., Mazeau, J., 1991. J. Phys. B 24, 1917.
Kazanski, A.K., Ostrovsky, V.N., 1993. Phys. Rev. A 48, R871.
Kazanski, A.K., Ostrovsky, V.N., 1994. J. Phys. B 27, 447.
Kazanski, A.K., Ostrovsky, V.N., 1995. Phys. Rev. A 51, 3698.
Keller, S., 2000. J. Phys. B 33, L513.
Ken-ichi Hino, shihara, T., Shimizu, F., Toshima, N., McGuire, J.H., 1993. Phys. Rev. A 48, 1271.
Kheifets, A., 2001. J. Phys. B 34, L247.
Kheifets, A., Bray, I., 1998a. Phys. Rev. A 57, 2590.
Kheifets, A., Bray, I., 1998b. Phys. Rev. Lett. 81, 4588.
Kheifets, A., Bray, I., 1998c. J. Phys. B 31, L447.
Kheifets, A., Bray, I., 2000. Phys. Rev. A 62, 065402.
Kheifets, A., Bray, I., Soejima, K., Danjo, A., Okuno, K., Yagishita, A., 1999. J. Phys. B 32, L501.
Knapp, A., Kheifets, A., Bray, I., Weber, Th., Landers, A.L., Schössler, S., Jahnke, T., Nickles, J., Kammer, S., Jagutzki, O., Schmidt, L.Ph., Osipov, T., Rösch, J., Prior, M.H., Schmidt-Böcking, H., Cocke, C.L., Dörner, R., 2002a. Phys. Rev. Lett. 89, 033004.
Knapp, A., Walter, M., Weber, Th., Landers, A.L., Schössler, S., Jahnke, T., Schöffler, M., Nickles, J., Kammer, S., Jagutzki, O., Schmidt, L.Ph.H., Osipov, T., Rösch, J., Prior, M.H., Schmidt-Böcking, H., Cocke, C.L., Feagin, J., Dörner, R., 2002b. J. Phys. B 35, L521.
Knudsen, H., Andersen, L.H., Hvelplund, P., Astner, G., Cederquist, H., Danared, H., Liljeby, L., Rensfelt, K.G., 1984. J. Phys. B 17, 3545.
Kopold, R., Becker, W., Rottke, H., Sandner, W., 2000. Phys. Rev. Lett. 85, 3781.
Kornberg, M.A., Miraglia, J.E., 1995. Phys. Rev. A 52, 2915.
Kossmann, H., Schmidt, V., Andersen, T., 1988. Phys. Rev. Lett. A 60, 1266.
Kossmann, H., Schwarzkopf, O., Kämmerling, B., Schmidt, V., 1989. Phys. Rev. Lett. 63, 2040.
Krässig, B., Dunford, R.W., Gemmell, D.S., Hasegawa, S., Kanter, E.P., Schmidt-Böcking, H., Schmitt, W., Southworth, S.H., Weber, Th., Young, L., 1999. Phys. Rev. Lett. 83, 53.
Kuchiev, M.Yu., 1987. Sov. Phys.—JETP Lett. 45, 404.
Lablanquie, P., Mazeau, J., Andric, L., Selles, P., Huetz, A., 1995. Phys. Rev. Lett. 74, 2192.
Lafon, R., Chaloupka, J.L., Sheehy, B., Paul, P.M., Agostini, P., Kulander, K.C., DiMauro, L.F., 2001. Phys. Rev. Lett. 86, 2762.
Lambropoulos, P., Maragakis, P., Zhang, J., 1998. Phys. Rep. 305, 203.
Larochelle, S., Talebpour, A., Chin, S.L., 1998. J. Phys. B 31, 1201.
Lein, M., Gross, E.K.U., Engel, V., 2000. Phys. Rev. Lett. 85, 4707.
Lein, M., Gross, E.K.U., Engel, V., 2001. Opt. Express 8, 441. http://www.opticsexpress.org/oearchive/source/30744.htm.
Levin, J.C., Lindle, D.W., Keller, N., Miller, R.D., Azuma, Y., Berrah Mansour, N., Berry, H.G., Sellin, I.A., 1991. Phys. Rev. Lett. 67, 968.
Levin, J.C., Armen, G.B., Sellin, I.A., 1996. Phys. Rev. Lett. 76, 1220.
Malegat, L., Selles, P., Huetz, A., 1997. J. Phys. B 30, 251.
Malegat, L., Selles, P., Kazansky, A.K., 2000. Phys. Rev. Lett. 85, 21.
Malegat, L., Selles, P., Kazansky, A.K., 2002. Phys. Rev. A 65, 032711.
Maulbetsch, F., Briggs, J.S., 1995. J. Phys. B 28, 551.
McGuire, J.H., 1997. Electron Correlation Dynamics in Atomic Collisions. Cambridge University Press, Cambridge.
Mergel, V., Achler, M., Dörner, R., Khayyat, Kh., Kambara, T., Awaya, Y., Zoran, V., Nyström, B., Spielberger, L., McGuire, J.H., Feagin, J., Berakdar, J., Azuma, Y., Schmidt-Böcking, H., 1998. Phys. Rev. Lett. 80, 5301.
Meyer, K.W., Bohn, J.L., Green, C.H., Esry, B.D., 1997. J. Phys. B 30, L641.
Moshammer, R., Feuerstein, B., Schmitt, W., Dorn, A., Schröter, C.D., Ullrich, J., Rottke, H., Trump, C., Wittmann, M., Korn, G., Hoffmann, K., Sandner, W., 2000. Phys. Rev. Lett. 84, 447.
Moshammer, R., et al., 2001. Phys. Rev. Lett. 87, 223201.
Moshammer, R., Feuerstein, B., Crespo Lopez Urrutin, I., Dorn, A., Fischer, D., Schröter, C.D., Schmitt, W., Ullrich, J., Rottke, H., Trump, C., Wittmann, M., Korn, G., Hoffmann, K., Sandner, W., 2002. Phys. Rev. A 65, 03541.
Pont, M., Shakeshaft, R., 1995a. Phys. Rev. A 51, 494.
Pont, M., Shakeshaft, R., 1995b. Phys. Rev. A 51, R2676.
Pont, M., Shakeshaft, R., 1996. Phys. Rev. A 54, 1448.
Reddish, T.J., Feagin, J., 1998. J. Phys. B 32, 2473.
Reddish, T.J., Wightman, J.P., MacDonald, M.A., Cvejanovic, S., 1997. Phys. Rev. Lett. 79, 2438.
Sacha, K., Eckhardt, B., 2001. Phys. Rev. 63, 043414.
Sagurton, M., Bartlett, R.J., Samson, J.A.R., He, Z.X., Morgan, D., 1995. Phys. Rev. A 52, 2829.
Samson, J.A.R., 1990. Phys. Rev. Lett. 65, 2861.
Samson, J.A.R., Green, C.H., Bartlett, R.J., 1993. Phys. Rev. Lett. 71, 201.

Samson, J.A.R., He, Z.X., Bartlett, R.J., Sagurton, M., 1994. Phys. Rev. Lett. 72, 3329.
Samson, J.A.R., Stolte, W.C., He, Z.X., Cutler, J.N., Lu, Y., Bartlett, R.J., 1998. Phys. Rev. A 57, 1906.
Schafer, K.J., Baorui Yang, DiMauro, L.F., Kulander, K.C., 1993. Phys. Rev. Lett. 70, 1599.
Scherer, N., Lörch, H., Schmidt, V., 1998. J. Phys. B 31, L817.
Schneider, T., Rost, J.M., 2003. Phys. Rev. A 67, 062704.
Schwarzkopf, O., Schmidt, V., 1995. J. Phys. B 28, 2847.
Schwarzkopf, O., Krässig, B., Elmiger, J., Schmidt, V., 1993. Phys. Rev. Lett. 70, 3008.
Schwarzkopf, O., Krässig, B., Schmidt, V., Maulbetsch, F., Briggs, J., 1994. J. Phys. B 27, L347–L350.
Selles, P., Malegat, L., Kazansky, A.K., 2002. Phys. Rev. A 65, 032711.
Shi, T.Y., Lin, C.D., 2002. Phys. Rev. Lett. 89, 163202.
Shingal, R., Lin, C.D., 1991. J. Phys. B 24, 251.
Soejima, K., Danjo, A., Okuno, K., Yagishita, A., 1999. Phys. Rev. Lett. 83, 1546.
Spielberger, L., Jagutzki, O., Dörner, R., Ullrich, J., Meyer, U., Mergel, V., Unverzagt, M., Damrau, M., Vogt, T., Ali, I., Khayyat, Kh., Bahr, D., Schmidt, H.G., Frahm, R., Schmidt-Böcking, H., 1995. Phys. Rev. Lett. 74, 4615.
Spielberger, L., Jagutzki, O., Krässig, B., Meyer, U., Khayyat, Kh., Mergel, V., Tschentscher, Th., Buslaps, Th., Bräuning, H., Dörner, R., Vogt, T., Achler, M., Ullrich, J., Gemmel, D.S., Schmidt-Böcking, H., 1996. Phys. Rev. Lett. 76, 4685.
Spielberger, L., Bräuning, H., Muthig, A., Tang, J.Z., Wang, J., Qui, Y., Dörner, R., Jagutzki, O., Tschentscher, Th., Honkimäki, V., Mergel, V., Achler, M., Weber, Th., Khayyat, Kh., Burgdörfer, J., McGuire, J., Schmidt-Böcking, H., 1999. Phys. Rev. 59, 371.
Surić, T., Pisk, K., Logan, B.A., Pratt, R.H., 1994. Phys. Rev. Lett. 73, 790.
Tang, J.Z., Shimamura, I., 1995. Phys. Rev. A 52, 1.
Teng, Z.J., Shakeshaft, R., 1994. Phys. Rev. A 49, 3597.
Ullrich, J., Moshammer, R., Berg, H., Mann, R., Tawara, H., Dörner, R., Euler, J., Schmidt-Böcking, H., Hagmann, S., Cocke, C.L., Unverzagt, M., Lencinas, S., Mergel, V., 1993. Phys. Rev. Lett. 71, 1697.
Viefhaus, J., Avaldi, L., Snell, G., Wiedenhöft, M., Hentges, R., Rüdel, A., Schäfer, F., Menke, D., Heinzmann, U., Engelns, A., Berakdar, J., Klar, H., Becker, U., 1996a. Phys. Rev. Lett. 77, 3975.
Viefhaus, J., Avaldi, L., Heiser, F., Hentges, R., Gessner, O., Rüdel, A., Wiedenhöft, M., Wielczek, K., Becker, U., 1996b. J. Phys. B 29, L729.
Walker, B., Sheehy, B., DiMauro, L.F., Agostini, P., Schafer, K.H., Kulander, K.C., 1994. Phys. Rev. Lett. 73, 1227.
Wannier, G.H., 1953. Phys. Rev. 90, 817.
Watson, J.B., Sanpera, A., Lappas, D.G., Knight, P.L., Burnett, K., 1997. Phys. Rev. Lett. 78, 1884.
Weber, T., 2003. http://hsbpc1.ikf.physik.uni–frankfurt.de/photonmolecule/D2.html, Dissertation, Johann Wolfgang Goethe Universiät, Frankfurt.
Weber, Th., Weckenbrock, M., Staudte, A., Spielberger, L., Jagutzki, O., Mergel, V., Urbasch, G., Vollmer, M., Giessen, H., Dörner, R., 2000a. J. Phys. B 33, L127.
Weber, Th., Weckenbrock, M., Staudte, A., Spielberger, L., Jagutzki, O., Mergel, V., Urbasch, G., Vollmer, M., Giessen, H., Dörner, R., 2000b. Phys. Rev. Lett. 84, 443.
Weber, Th., Giessen, H., Weckenbrock, M., Staudte, A., Spielberger, L., Jagutzki, O., Mergel, V., Urbasch, G., Vollmer, M., Dörner, R., 2000c. Nature 404, 608.
Weber, T., Jagutzki, O., Hattass, M., Staudte, A., Nauert, A., Schmidt, L., Prior, M.H., Landers, A.L., Bräuning-Demian, A., Bräuning, H., Cocke, C.L., Osipov, T., Ali, I., Diez Muino, R., Rolles, D., Garcia de Abajo, F.J., Fadley, C.S., Van Hove, M.A., Cassimi, A., Schmidt-Böcking, H., Dörner, R., 2001a. J. Phys. B 34, 3669.
Weber, Th., Weckenbrock, M., Staudte, A., Hattass, M., Spielberger, L., Jagutzki, O., Mergel, V., Urbasch, G., Schmidt-Böcking, H., Giessen, H., Bräuning, H., Cocke, C., Prior, M., Dörner, R., 2001b. Opt. Express 7(9) 368. http://www.opticsexpress.org/oearchive/source/30623.htm.
Weckenbrock, M., 2001. Diploma Thesis, J.W. Goethe University, Frankfurt/Main.
Weckenbrock, M., Hattass, M., Czasch, A., Jagutzki, O., Schmidt, L., Weber, T., Roskos, H., Löffler, T., Thomson, M., Dörner, R., 2001. J. Phys. B 34, L449.
Wightman, J.P., Cveejanovic, S., Reddish, T.J., 1998. J. Phys. B 31, 1753.
Witzel, B., Papadogiannis, N.A., Charalambidis, D., 2000. Phys. Rev. Lett. 85, 2268.
Ya Amusia, M., Drukarev, E.G., Krivec, R., Mandelzweig, V.B., 2002. Phys. Rev. A 66, 052706.